Molecular Therapy
Original Article

Targeted genomic translocations and inversions generated using a paired prime editing strategy

Jiyeon Kweon,[1,2,4] Hye-Yeon Hwang,[3,4] Haesun Ryu,[3] An-Hee Jang,[1,2] Daesik Kim,[3] and Yongsub Kim[1,2]

[1]Department of Biomedical Sciences, Asan Medical Institute of Convergence Science and Technology, Asan Medical Center, University of Ulsan College of Medicine, Seoul 05505, Republic of Korea; [2]Stem Cell Immunomodulation Research Center, University of Ulsan College of Medicine, Seoul 05505, Republic of Korea; [3]Department of Precision Medicine, Sungkyunkwan University School of Medicine, Suwon 16419, Republic of Korea

A variety of cancers have been found to have chromosomal rearrangements, and the genomic abnormalities often induced expression of fusion oncogenes. To date, a pair of engineered nucleases including ZFNs, TALENs, and CRISPR-Cas9 nucleases have been used to generate chromosomal rearrangement in living cells and organisms for disease modeling. However, these methods induce unwanted indel mutations at the DNA break junctions, resulting in incomplete disease modeling. Here, we developed prime editor nuclease-mediated translocation and inversion (PETI), a method for programmable chromosomal translocation and inversion using prime editor 2 nuclease (PE2 nuclease) and paired pegRNA. Using PETI method, we successfully introduced DNA recombination in episomal fluorescence reporters as well as precise chromosomal translocations in human cells. We applied PETI to create cancer-associated translocations and inversions such as *NPM1-ALK* and *EML4-ALK* in human cells. Our findings show that PETI generated chromosomal translocation and inversion in a programmable manner with efficiencies comparable of Cas9. PETI methods, we believe, could be used to create disease models or for gene therapy.

INTRODUCTION

Chromosomal rearrangements, including deletions, inversions, duplications, and translocations, are chromosome abnormalities that are induced mainly by the generation of DNA double-strand breaks (DSBs) at two different locations, followed by the rejoining of the DNA ends in a new configuration.[1] These structural variations are frequently identified in various types of cancers and are often the underlying cause of tumorigenesis.[2,3] To elucidate the effects of such rearrangements, previous studies have introduced targeted chromosomal rearrangements in cells and organisms using a pair of programmable nucleases including zinc finger nucleases, TAL effector nucleases, and CRISPR-Cas9 nucleases.[4–11] In particular, Cas9 nuclease with paired guide RNAs (gRNAs) has been used to generate cancer-associated chromosomal rearrangements, such as *EML4-ALK*, *NPM-ALK*, *CD74-ROS1*, *KIF5B-RET*, *EWSR1-FLI1*, and *AML1-ETO*.[10–12] Two gRNAs targeting two chromosomes can lead to chromosomal translocation by generating DNA DSBs on each chromosome, However, Cas9-mediated translocations are accompanied by additional indel mutations at the fragment junctions, and it is difficult to generate precise translocation or to insert or delete desired sequences at the junction.

Prime editor 2 (PE2) enables the generation of genetic modifications, including all types of substitutions, small insertions, and deletions, as well as combinations of these mutations, at target sites without the formation of DNA double-strand breaks in cultured cells and whole organisms.[13–21] PE2 consists of Cas9 H840A nickase fused to an engineered Moloney murine leukemia virus reverse transcriptase (RT) and a prime editing guide RNA (pegRNA) that includes a spacer sequence, a primer binding sequence (PBS), and an RT template (RTT) sequence containing the desired edit. Prime editing is composed of (1) the generation of a single-strand break in the non-target strand via Cas9 H840A nickase, (2) hybridization of the PBS in the pegRNA to the 3′ end of the nicked strand, making a DNA/RNA complex; (3) RT-mediated DNA extension of the nicked strand according to the RTT sequence, which generates a 3′-flap containing the intended edit sequence; and (4) incorporation of the 3′-flap sequence into the genome. Prime editing activities are improved by using an additional nicking guide RNA, which leads to the generation of a nick in the non-edited strand.

Recently, advanced prime editor (PE)-based methods, known as Prime-Del[22] and PE-Cas9-based deletion and repair (PEDAR),[23] have been developed to induce large deletions of up to 10 kb. Both methods involve a pair of pegRNAs targeting opposite strands; in Prime-Del, the pegRNAs are used together with PE2, whereas in

Received 13 May 2022; accepted 12 September 2022;
https://doi.org/10.1016/j.ymthe.2022.09.008.

[4]These authors contributed equally

Correspondence: Daesik Kim, Department of Precision Medicine, Sungkyunkwan University School of Medicine, Suwon 16419, Republic of Korea.
E-mail: dskim89@skku.edu
Correspondence: Yongsub Kim, Department of Biomedical Sciences, Asan Medical Institute of Convergence Science and Technology, Asan Medical Center, University of Ulsan College of Medicine, Seoul 05505, Republic of Korea.
E-mail: yongsub1.kim@gmail.com

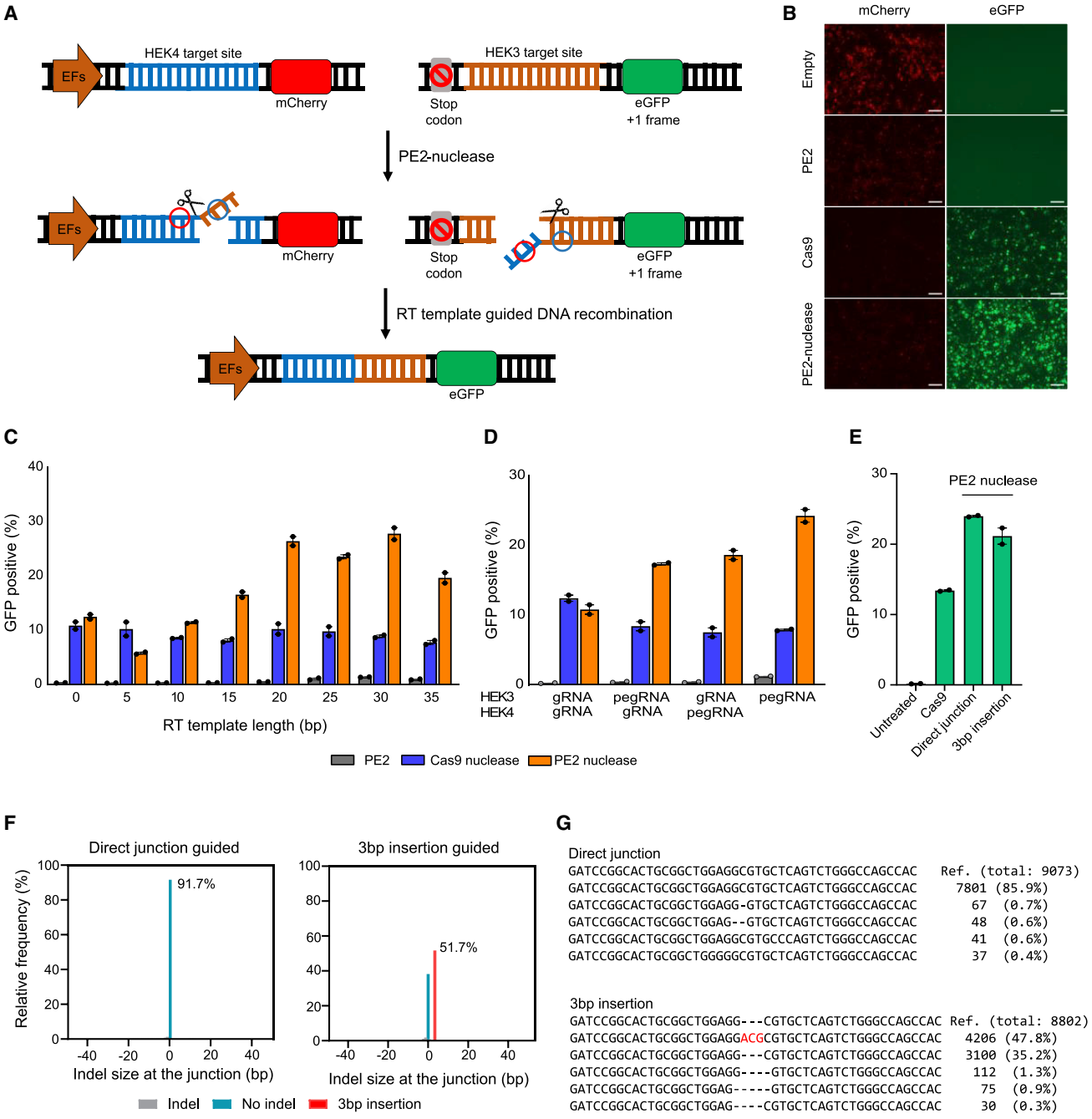

Figure 1. PETI-mediated translocation in an episomal fluorescent reporter

(A) Overview of the PETI method for generating episomal DNA recombination in human cells. The paired pegRNAs target the HEK3 and HEK4 sites that are incorporated into the two plasmids that make up the episomal fluorescent reporter system. PETI induces the formation of 3′-flaps at each of the target sites, which are complementary to sequences at the other target site, resulting in episomal translocations. (B) Representative fluorescence microscope images showing the absence or presence of eGFP expression, which results from episomal translocations potentially induced by PE2, PE2 nuclease, or Cas9 nuclease. Scale bar represents 100 μM. (C) Effects of 3′-flap length on translocation outcomes. Cells were transfected with plasmids encoding PE2, PE2 nuclease, or Cas9 nuclease and pegRNAs that generated 3′-flaps of different lengths (0–35 bp, increasing in increments of 5 bp), and the percentage of GFP-positive cells was evaluated using fluorescence-activated cell sorting. (D) Effects of combinations of pegRNA and gRNA on translocation outcomes. Cells were transfected with plasmids encoding PE2, PE2 nuclease, or Cas9 nuclease and pegRNA or gRNA pairs, and the GFP-positive cells were evaluated using fluorescence-activated cell sorting. (E) Cells were transfected with plasmids encoding Cas9 nuclease with gRNAs or PE2 nuclease

(legend continued on next page)

PEDAR, they are used with a Cas9 nuclease-RT fusion, here referred to as PE2 nuclease. We reasoned that prime editing systems based on paired pegRNAs could be used to induce not only large deletions but also other chromosomal structural rearrangements like translocations and inversions. Here, we developed the PE2 nuclease-based translocation and inversion (PETI) method, which uses PE2 nuclease and paired pegRNAs to induce programmable translocations and inversions in mammalian cells with high efficiency and purity.

RESULTS

DNA recombination induced by PETI using a fluorescent reporter system

To test the feasibility of using the PETI strategy to induce programmed DNA recombination, we designed two plasmids encoding fluorescent reporters. The first contains a promoter, a HEK4 target site, and the mCherry gene, and the second contains a stop codon, a HEK3 target site, and the eGFP gene. Because the eGFP gene lacks a promoter, reporter-transfected cells can express mCherry but not eGFP (Figure 1A). When PETI induces DNA recombination between the HEK4 and HEK3 target sites of these two plasmids in cells, the promoter moves in front of the eGFP gene, resulting in eGFP expression (Figure 1A). We constructed paired pegRNAs to induce this recombination using the PETI system. The pegRNA that targets the HEK4 site generates a 3′-flap containing the desired sequence (blue circle in Figure 1A), which is complementary to the HEK3 target site at the recombination junction; the pegRNA that targets the HEK3 site generates a 3′-flap that is complementary to the HEK4 target at the recombination junction (Figure 1A, red circle). In contrast to the low expression of eGFP observed when HEK293T cells were transfected with plasmids encoding PE2 and the paired pegRNAs, transfection of plasmids encoding PE2 nuclease and the paired pegRNAs induced higher eGFP expression (Figure 1B). Cas9 nuclease and paired single guide RNAs (sgRNAs) targeting the HEK3 and HEK4 target sites also induced eGFP expression (Figure 1B). Note that PE2, which induces extremely low indel mutations, significantly reduced mCherry expression, because the PE2 protein and the pegRNA complex that bound between the promoter and the mCherry coding sequence could block RNA polymerase elongation. The length of the RTT in the paired pegRNAs targeting the HEK4 and HEK3 sites was then changed from 0 to 35 bp in 5 bp increments to generate 3′-flaps of different lengths; plasmids encoding each of the new pegRNA pairs were transfected with plasmids encoding PE2, PE2 nuclease, or Cas9 nuclease. The length of the 3′ extension did not affect Cas9 nuclease-mediated DNA recombination activity, whereas the frequency of PE2 nuclease-mediated recombination increased as the length of the 3′-flap was gradually increased from 0 to 20 bp, but there was no significant change when it was increased from 20 to 35 bp (Figure 1C). Using the fluorescent reporter, we then investigated the synergistic effects of paired 3′-flaps (Figures 1A and 1D). Transfection of plasmids encoding PE2 nuclease and paired pegRNAs resulted in higher DNA recombination frequencies than those induced by PE2 nuclease, a single pegRNA, and sgRNA (Figure 1D), indicating that paired 3′-flaps have a synergistic effect.

To examine the accuracy of the PETI strategy for DNA recombination, we further constructed paired pegRNAs inducing 3 bp (5′-ACG-3′) insertion at the recombination. We first conducted flow cytometry assays to measure the recombination efficiency and found that both paired pegRNAs (direct junction guided and 3 bp insertion guided) induced DNA recombination with comparable efficiency (Figure 1E). Targeted deep sequencing showed that PE2 nuclease with paired pegRNAs inducing direct junction induced DNA recombination with a higher accuracy than Cas9 nuclease (91.7% for PE2 nuclease, 62.8% for Cas9 nuclease) (Figures 1F and S1). Furthermore, we found that paired pegRNAs inducing 3 bp (5′-ACG-3′) insertion at the junction could induced the insertional mutation in episomal reporter plasmids (51.7%) as well as reporter integrated cell line (76.9%) (Figures 1F, 1G, and S2). Although episomal reporter assays may overestimate the efficiency of rearrangements because of the use of multiple copies of plasmids in a single cell, these results showed that PETI indeed induce DNA recombination in a precise and programmable manner.

PETI induces chromosomal translocations in genomic DNA

We next investigated whether PETI induces precise chromosomal translocation between endogenous loci in human cells. We co-transfected plasmids encoding paired pegRNAs for inducing reciprocal translocations between the HEK3 and HEK4 genomic sites and PE2 or PE2 nuclease into HEK293T cells (Figure 2A). For a positive control, we also co-transfected plasmids encoding Cas9 nuclease and sgRNAs targeting the HEK3 and HEK4 sites. We then amplified the expected translocation junctions with reciprocal translocation-specific primer pairs and found that translocations were induced in cells transfected with plasmids encoding PE2 nuclease and paired pegRNAs, as well as Cas9 nuclease and dual sgRNAs, but not in cells transfected with plasmids encoding PE2 and paired pegRNAs (Figure S3A). We analyzed these amplicons by targeted deep sequencing and found that PE2 nuclease induced more precise reciprocal translocation than Cas9 nuclease (43.9% and 23.9% with PE2 nuclease; 11.0% and 0% with Cas9 nuclease at each junction) (Figures 2B–2D). Following this experiment, we designed paired pegRNAs to induce a 3 bp deletion or a 4 or 5 bp insertion (containing an EcoRI or BamHI site) at the junction of the reciprocal translocation and transfected plasmids encoding the pegRNAs and PE2 or PE2 nuclease or Cas9 nuclease and sgRNAs. Translocation junctions were also amplified translocation-specific primer pairs in the presence of PE2 nuclease with these paired pegRNAs. The amplified junction generated by paired pegRNAs designed to insert an EcoRI or

with two types of pegRNA pairs (direct junction guided or 3 bp insertion guided), and the GFP-positive cells were evaluated using fluorescence-activated cell sorting. Data are presented as mean ± SEM (n = 2 biologically independent samples). (F) The relative frequency of sequence reads of amplicons generated using translocation-specific primers. Direct translocation and PETI-guided translocation (3 bp insertion) are shown in blue and red bars, respectively. (G) Results of targeted sequencing of amplicons generated using translocation-specific primers.

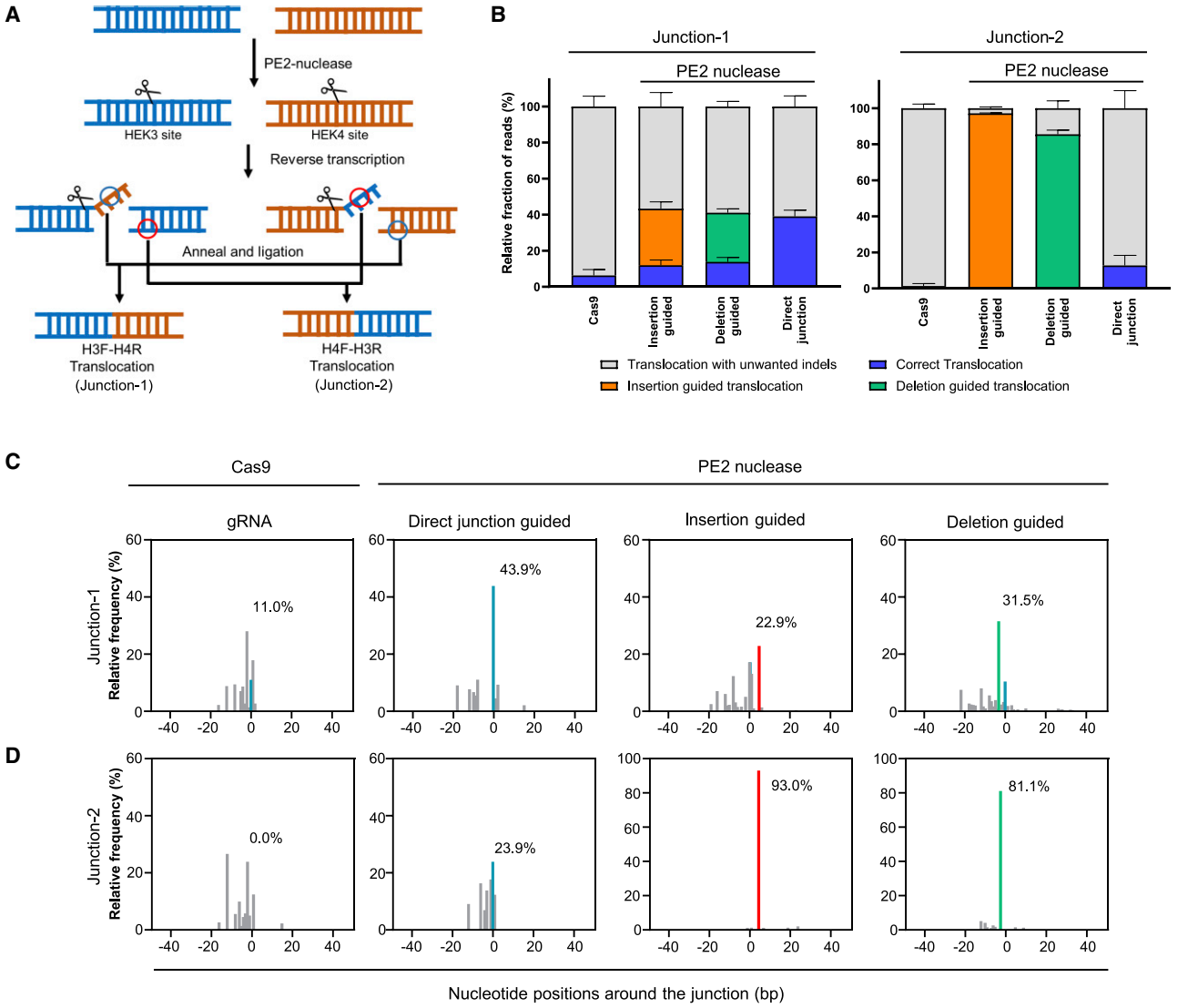

(legend on next page)

BamHI site was digested by EcoRI or BamHI, respectively but that the junction generated by Cas9 nuclease was not (Figure S3B). We then used deep sequencing of PCR-amplified translocation junctions to validate the editing accuracy. At both reciprocal translocation junctions, we revealed that PE2 nuclease was more accurate than Cas9 nuclease (Figures 2C and 2D). The translocation frequencies were also measured by dilution PCR,[5,24] and we found that PE2 nuclease induced reciprocal translocation with a similar frequency to Cas9 nucleases (Table 1; Figure S4). These results indicated that PE2 nuclease with appropriate paired pegRNAs can induce reciprocal translocations with desired mutations at the junctions in human cells.

In general, when two DSBs are induced simultaneously in different chromosomes, translocations could cause four different types of genomic rearrangements[25] (Figure S5). Possible rearrangements include not only reciprocal translocations but also unusual results such as dicentric and acentric chromosomes. Cas9 and PE2 nuclease, which induce DNA DSBs in the genome, could potentially generate not only reciprocal translocations but also unusual translocations resulting in dicentric and acentric chromosomes. We used multiplex PCR and deep sequencing to detect all types of translocations, amplifying not only reciprocal translocation junctions but also junctions formed by unusual translocations as well as un-translocated DNA (Figure 2E). Although multiplex PCR-based assay cannot detect precise translocation frequencies because it depends on target-specific primers, the assay can be used to detect the relative frequency of each translocation as well as translocation accuracies at their junctions. Our multiplex PCR-based assay revealed that compared with Cas9 nuclease, PE2 nuclease increased the relative frequency of desired translocations while decreasing the frequency of unwanted translocations (Figure 2F). In addition to inducing chromosomal rearrangements, Cas9 and PE2 nucleases were also capable of inducing DSBs at their on- and off-target sites, which results in unintended off-target indel mutations. Targeted deep sequencing was used to elucidate the unwanted off-target mutation, and we found that PE2 nuclease, compared with Cas9, reduced indel frequencies at their on- and off-target sites (Figure S6). We also measured translocation frequencies between HEK3 on-target site and HEK4 off-target sites by dilution PCR and found that PETI decreased unwanted translocation compared with Cas9 (Table 1; Figure S7). These results demonstrated that PETI generate the desired translocations with higher efficiency and purity than Cas9.

Generation of a cancer-associated translocation using PETI

Anaplastic lymphoma kinase (*ALK*) gene fusion induced by chromosomal translocation or inversion is well-known driving mutation underlying the development of various type of cancers such as lung adenocarcinoma, non-small cell lung carcinoma, and inflammatory myofibroblastic tumor.[26] We first chose two types of *ALK* gene fusion, *NPM1-ALK* and *KIF5B-ALK*, generated by reciprocal translocation (Figures 3A and 3B). We generated paired pegRNAs that target *ALK* and either *NPM1* or *KIF5B* to induce these translocations. In case of *NPM1-ALK* fusion, the *ALK*-targeting pegRNA produces 3′-flaps that are complementary to *NPM1*, and the *NPM1*-targeting pegRNA produces 3′-flaps that are complementary to *ALK*. The pegRNAs were designed to insert a 5 bp (*ALK*-targeting pegRNA) or a 6 bp (*NPM1*-targeting pegRNA) insertion at the chromosomal translocation junctions. In case of *KIF5B-ALK* fusion, the pegRNA targeting *ALK* produces 3′-flaps that are complementary to *KIF5B*, and pegRNA targeting *KIF5B* generate 3′-flaps that are complementary to *ALK*.

We then co-transfected HEK293T cells with plasmids encoding PE2, PE2 nuclease, or positive control Cas9 nuclease, as well as the paired pegRNAs, and investigated the resulting translocations using primers that amplify the translocation junctions. Unlike PE2, both Cas9 and PE2 nuclease could cause reciprocal translocations (Figures S8A and S8B). We conducted targeted deep sequencing using translocation-specific primer pairs and found that PETI induced a significantly higher fraction of desired translocations with the intended insertion at the *NPM1-ALK* and *KIF5B-ALK* junctions (Figures 3C–3E). To further our understanding of these outcomes, we used multiplex PCR, as described above, and revealed that PE2 nuclease induced precise translocations with PETI-guided manner and reduced undesired translocation compared with Cas9 nuclease (Figure 3F).

To determine if the generated *NPM1-ALK* gene fusions were transcribed, we isolated mRNA from the transfected cells described above and performed reverse transcription PCR (RT-PCR) using primers amplifying the translocation junction. The presence of a PCR amplicon showed that the *NPM1-ALK* fusions induced by both the Cas9 and PE2 nuclease-mediated translocations were transcribed (Figure S8C). We conducted dilution PCR to measure translocation frequencies of *NPM1-ALK* and *KIF5B-ALK* and found that PE2 nuclease induced the reciprocal translocations with higher frequencies compared with Cas9 (Table 1; Figure S9). We also co-transfected

Figure 2. PETI-mediated translocation at an endogenous genomic locus

(A) Representative schematic showing PETI-mediated translocations at endogenous target sites. PETI induces the formation of 3′-flaps at each of the target sites, which are complementary to sequences at the other target site, resulting in translocations. (B) Targeted sequencing of amplicons generated using translocation-specific primers. The bar charts represent the fraction of reads with direct translocations (blue), translocations with the intended insertion (orange) or deletion (green), and translocations with unwanted indels (gray). (C and D) Representative results of relative frequency of sequence reads in PCR amplicons amplified by translocation-specific primers, either H3F (HEK3 forward) and H4R (HEK4 reverse) or H4F and H3R. Direct translocation and PETI-induced translocation are indicated by blue and red bars, respectively. (E) Schematic overview of multiplex PCR to detect PE2-, PE2 nuclease-, or Cas9 nuclease-mediated translocations. Un-translocated genomic DNA is amplified by primers T1F and T1R or T2F and T2R, the junctions of desired translocations are amplified by T1F and T2R or T2F and T1R, and the junctions of undesired translocations are amplified by T1F and T2F or T2R and T1R. (F) Fraction of sequencing reads of multiplex PCR amplicons generated from desired and undesired PE2-, PE2 nuclease-, or Cas9 nuclease-mediated translocations. Data are presented as mean ± SEM (n = 3 biologically independent samples).

Table 1. Estimated frequencies of Cas9- or PETI-mediated chromosomal translocations and inversions

			Junction-1			Junction-2		
Target sites	Target rearrangements	Types	Lower, %	Estimated, %	Upper, %	Lower, %	Estimated, %	Upper, %
HEK3-HEK4	Translocation	Cas9	0.10	0.18	0.33	0.22	0.37	0.61
		insertion guided	0.07	0.13	0.25	0.31	0.50	0.80
		deletion guided	0.04	0.08	0.18	0.41	0.66	1.06
		direct junction guided	0.07	0.14	0.27	0.11	0.20	0.36
HEK3-HEK4-OFF-1	Translocation	Cas9	0.14	0.26	0.51	0.18	0.36	0.72
		PE2 nuclease	0.02	0.05	0.10	0.05	0.11	0.24
HEK3-HEK4-OFF-2	Translocation	Cas9	0.11	0.20	0.38	0.14	0.26	0.48
		PE2 nuclease	0.02	0.03	0.07	0.03	0.06	0.12
NPM1-ALK	Translocation	Cas9	0.04	0.08	0.17	0.07	0.14	0.29
		PE2 nuclease	1.00	2.00	4.00	0.19	0.37	0.72
KIF5B-ALK	Translocation	Cas9	0.04	0.07	0.14	0.04	0.08	0.16
		PE2 nuclease	0.07	0.13	0.26	0.04	0.08	0.16
EML4-ALK-V1	Inversion	Cas9	0.21	0.45	0.97	0.26	0.54	1.13
		PE2 nuclease	0.65	1.26	2.45	0.87	1.87	4.02
EML4-ALK-V2	Inversion	Cas9	0.85	1.80	3.86	2.57	5.20	10.6
		PE2 nuclease	5.24	10.1	19.6	5.74	11.6	23.3
EML4-ALK-V3	Inversion	Cas9	0.36	0.71	1.44	0.20	0.44	0.94
		PE2 nuclease	0.87	1.87	4.02	0.33	0.67	1.36

plasmids encoding PE2 nuclease or positive control Cas9 nuclease, as well as the paired pegRNAs to induce *NPM1-ALK* and *KIF5B-ALK* translocation in A549 lung cancer cell line and performed targeted deep sequencing using PCR product, which amplifies the translocation junctions using translocation-specific primer pairs. Sequencing results indicated that PETI induced a PETI-guided translocation and direct translocation better than Cas9 nuclease (Figure S10A), which is similar to that performed in HEK293T cells. These findings indicate that PETI can be used to produce cancer-related chromosomal translocations with high fidelity.

Generation of cancer-associated inversions using PETI

Next, we asked whether PETI could be used to generate cancer-associated inversions in endogenous genomes. One of the most common oncogenic chromosomal rearrangements in human cancers, particularly non-small cell lung cancers, leads to the expression of *EML4-ALK* fusion proteins. There are several *EML4-ALK* fusion protein variants, which are produced as a result of paracentric inversions within the short arm of chromosome 2 (Figure 4A). *EML4-ALK* variants 1, 2, and 3 (V1, V2, and V3) account for more than 90% of oncogenic *EML4-ALK* variants (Figure 4B).[27] We first designed paired pegRNAs targeting intron 19 of the *ALK* gene and intron 13 of the *EML4* gene to induce an inversion resulting in *EML4-ALK* V1 and then transfected HEK293T cells with plasmids encoding PE2, PE2 nuclease, or Cas9 and the appropriate pegRNAs. When HEK293T cells were treated with plasmids encoding Cas9 or PE2 nuclease and paired pegRNAs, inversions were detected using inversion-specific PCR, however, PE2 and paired pegRNAs did not cause inversion (Figure S11A). Next, we generated pegRNAs to generate the inversions expected to result in the oncogenic fusions *EML4-ALK* V2 and V3. We transfected HEK293T with plasmids encoding these paired pegRNAs or sgRNAs and PE2, PE2 nuclease, or Cas9. Inversions were induced by PE2 nuclease and Cas9 nuclease but not by PE2, which was consistent with the results of the experiment involving *EML4-ALK* V1 (Figure S11A). Next, we performed targeted amplicon sequencing of PCR products generated by inversion-specific primers and indicated that PETI produced a higher ratio of correct inversions and inversions with the intended insertion than Cas9 (Figures 4C and 4D). We then used multiplex PCR and deep sequencing to determine the relative frequency of inversion and found that the frequencies generated by PE2 nuclease are significantly higher than those of Cas9 in three types of *EML4-ALK* inversion (Figure 4E). Using dilution PCR, we revealed that PETI could induce *EML4-ALK* V2 inversion by 10.1% and 11.6% at junction-1 and junction-2, respectively (Table 1; Figure S12). We also induced PETI-mediated inversion in A549 cells and found that PE2 nuclease could induce a higher fraction of PETI-guided inversion and direct inversion compared with Cas9 nuclease (Figure S10B).

To investigate whether the PETI- and Cas9 nuclease-induced *EML4-ALK* transcripts were expressed, we isolated total mRNA from the transfected cells described above and performed RT-PCR. We confirmed that PETI and Cas9 nuclease, but not PE2, led to the expression of *EML4-ALK* transcripts via paracentric inversion (Figures 4F and S11B). In addition, we further conducted a flow cytometric assay to quantify *ALK* protein expression at the single cell

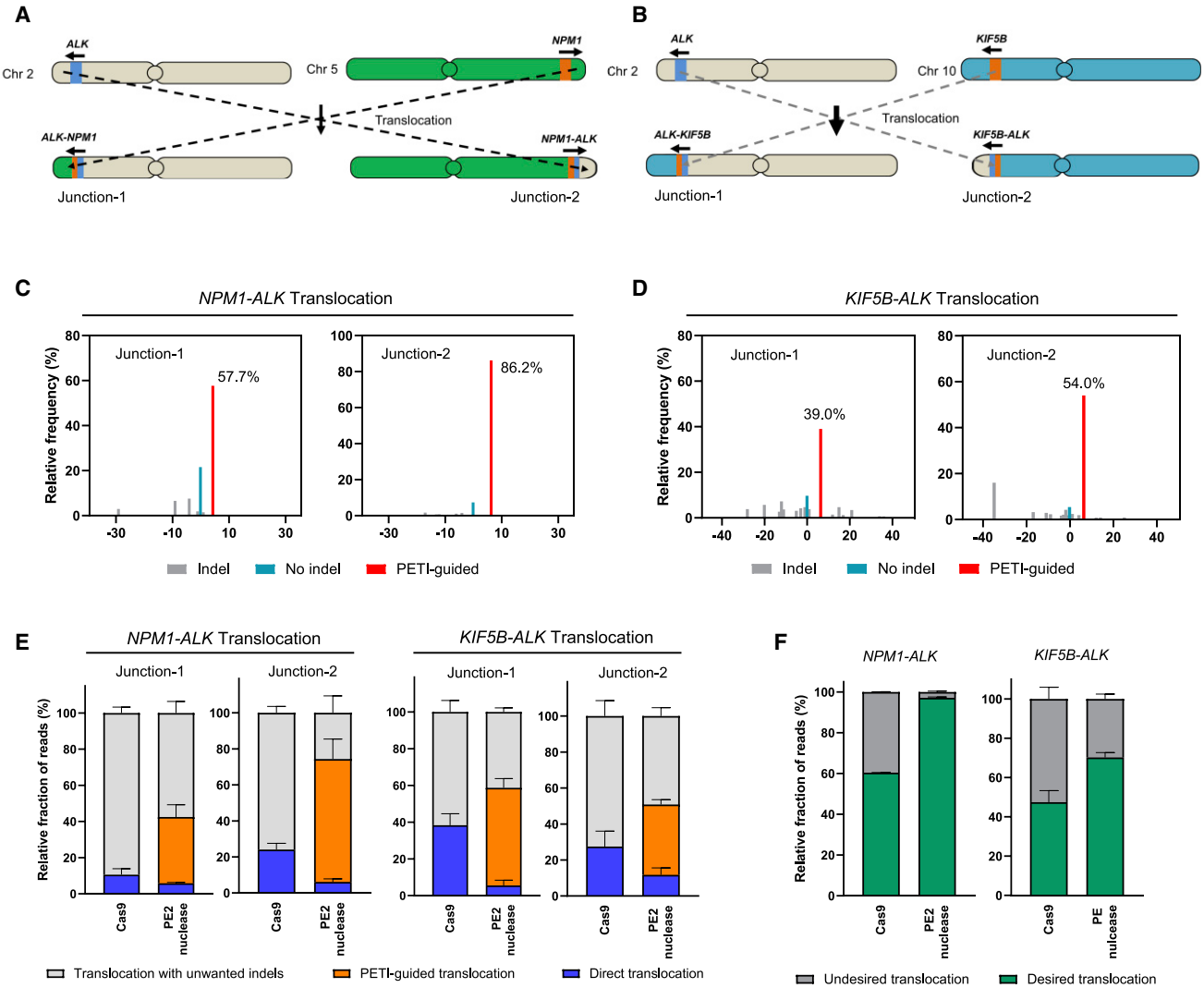

Figure 3. Use of PETI to generate a cancer-associated translocation

(A and B) Schematic of the chromosomes before and after the reciprocal translocations generating the *NPM1-ALK* (a) and *KIF5B-ALK* fusion (b). (C and D) Representative results of relative frequency of sequence reads in PCR amplicons amplified by translocation-specific primers amplifying either junction-1 or junction-2. (E) Targeted deep sequencing of amplicons generated using translocation-specific primers. The bar charts represent the fraction of reads with direct translocations (blue), PETI-guided translocations (orange), and translocations with unwanted indels (gray). (F) Fraction of sequencing reads of multiplex PCR amplicons generated from desired and undesired PE2-, Cas9 nuclease-, and PE2 nuclease-mediated translocations. Data are presented as mean ± SEM (n = 3 biologically independent samples).

level[10] and observed increased *ALK* expression in Cas9 or PE2 nuclease treated cells (Figures 4G and 4H). These results suggested that PETI can be used to generate cancer-associated inversions with high frequency and fidelity.

DISCUSSION

Here, we describe PETI, a simple and accurate method for inducing targeted translocations and inversions in programmable manner using PE2 nuclease and paired pegRNAs. First, we showed that PETI could induce programmed DNA recombination in episomal plasmid of reporter constructs and reporter integrated stable cell lines. Subsequently, we used PETI to induce accurate translocations containing the desired sequences in the genomes of human cells. Finally, we generated precise cancer-associated translocations (*NPM1-ALK* and *KIF5B-ALK* fusions) and inversions (*EML4-ALK* fusion variants) using PETI.

Although PETI enables programmable genomic rearrangements in living cells, challenges remain to improve the performance of PETI. As the prime editing efficiency depends on the activity of pegRNAs, the efficiency and accuracy of PETI may be closely related to the composition pegRNAs in a site-specific manner. Indeed, the length

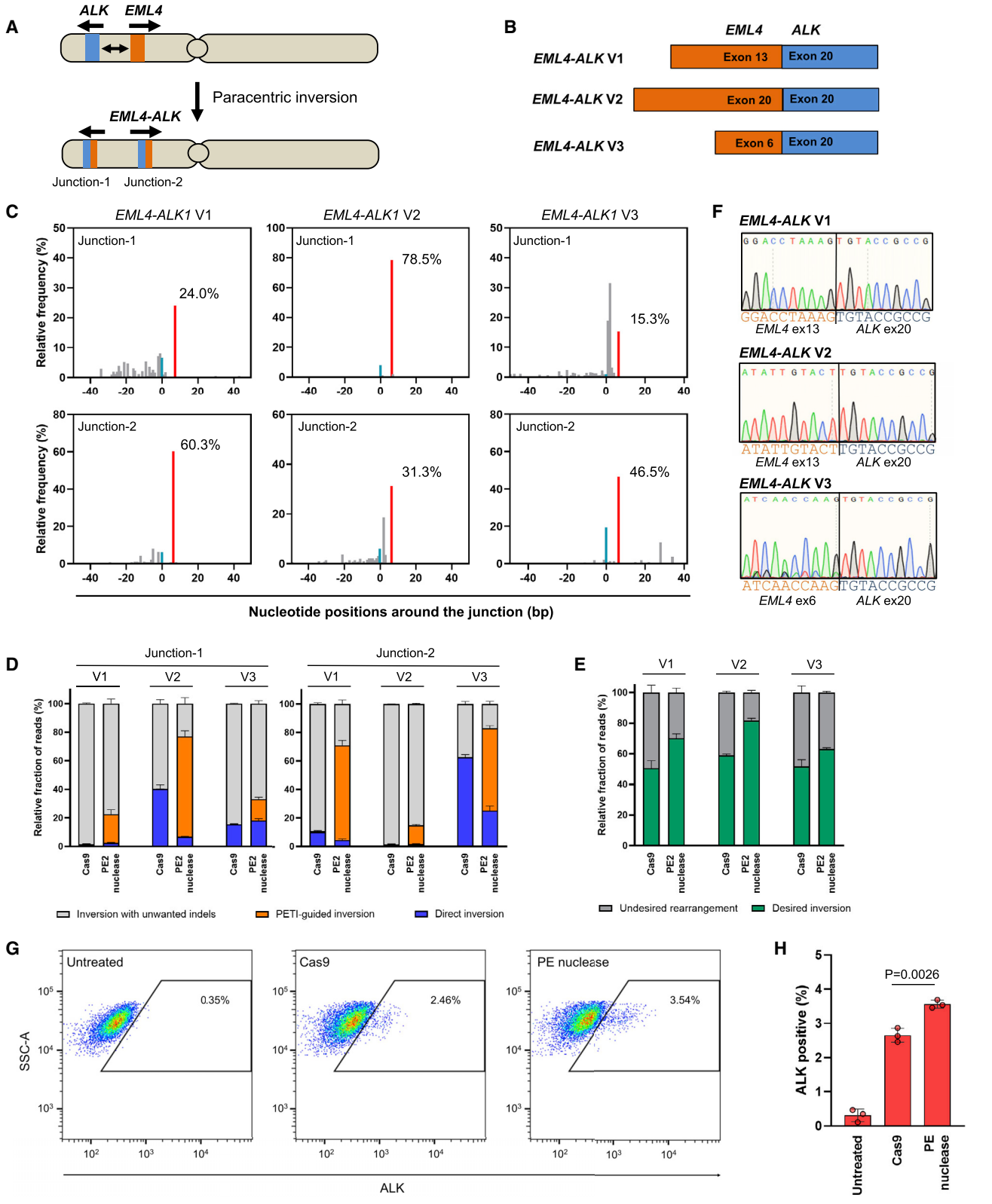

(legend on next page)

of RTT affected the accuracy of PETI with different trends at the two target sites (Figure S13). Therefore, optimization of pegRNAs for each target locus is required to improve the performance of PETI.

Although previous papers have reported that Cas9 with a pair of gRNAs could induce inversions and translocations in living system, we believe that PETI has several advantages over Cas9. Cas9 frequently generate indels at the rearranged genomic breakpoint junctions.[8] The majority of disease-associated genomic breakpoints occur in intron region indels at these sites do not affect protein expression, but genomic rearrangements between exon regions are found in tumors such as *NAB2-STAT6* fusions,[28] and precise editing by PETI might be required to disease modeling and therapeutic approach. PETI can also reduce undesired genomic rearrangement between genomic breakpoint junctions, thereby decreasing unwanted mutations in the genome compared Cas9 nuclease. Furthermore, PETI can install or remove specific sequences at the rearranged genomic breakpoint junctions. As well as small size of 3–6 bp insertion, PETI can introduce an attP sequence of 40 bp at the breakpoint junction (Figure S14). This programmable characteristic of PETI offers opportunities for further applications such as gene tagging and insertion of epitope sequences.

Newly developed prime editing technologies such as Prime-Del, PEDAR, and twinPE can produce large chromosomal deletions or inversions.[22,23,29] Prime-Del use PE2 with a paired pegRNAs and PEDAR use PE2 nuclease (PE-Cas9) with a paired pegRNAs for targeted genomic deletion up to ~10 kb. Although PETI is similar to PEDAR in that it uses PE2 nuclease, PETI enables large-scale genome rearrangement in living cells. Another method, called twinPE, uses PE2 with a paired pegRNAs and Bxb1 recombinase to generate chromosomal deletions and inversions.[29] To induce inversions using this method, Bxb1 recognition sites attB and attP (39 and 50 bp, respectively) are first inserted into the genome and then, Bxb1 recombinase induces DNA recombination at attB and attP sites, resulting in deletions or inversions. Although twinPE provides precise deletions and inversions without unwanted DNA cleavage, it requires four pegRNAs (a paired pegRNAs for attB insertion and a paired pegRNAs for attP insertion) and additional Bxb1 recombinase. In addition, inversions generated using twinPE contain attB and attP sequences at the inversion junction. In contrast, the PETI method does not leave a scar at such junctions and can even insert or remove specific bases. On the basis of these results, we anticipate that PETI-mediated chromosomal rearrangements will be a powerful approach for not only generating but also correcting disease-associated inversions and translocations.

MATERIALS AND METHODS

Plasmid construction

The pCMV-PE2 (Addgene plasmid #132775) and pU6-pegRNA-GG-acceptor (Addgene plasmid #132777) plasmids were a gift from David Liu. pegRNA-encoding plasmids were generated by Golden Gate assembly using a custom acceptor plasmid according to methods described in a previous paper (Table S1).[30] pCMV-PE2 was modified to encode pCMV-PE2 nuclease by reverting the H840A mutation in the Cas9 sequence to H840 using a Q5 Site-Directed Mutagenesis Kit (New England Biolabs). The coding sequences of eGFP and mCherry were cloned into pUC19 and p3s backbones, respectively, to generate pUC19-TL-eGFP and p3s-TL-EFS-mCherry plasmids for the episomal reporter assay. pLX-sgRNA (Addgene plasmid #50662) was used to make viral vector of these reporter constructs, pLX-TL-mcherry and pLX-TL-eGFP. Briefly, pLX-sgRNA vector was digested BamHI and NheI restriction enzyme and reporter constructs were cloned into them by Gibson Assembly. pLX-TL-mcherry vector was obtained by further changing blasticidin markers to puromycin markers.

Human cell culture and transfection

HEK293T cells (American Type Culture Collection [ATCC] CRL-11268) were maintained in DMEM supplemented with 10% fetal bovine serum and 1% penicillin/streptomycin and verified using an STR profile. For the episomal reporter assay, HEK293T cells were seeded onto 48-well plates and transfected with 500 ng of plasmid (50 ng each of the pUC19-TL-eGFP and p3s-TL-EFS-mCherry plasmids, 200 ng of PE2-, PE2 nuclease-, or Cas9-encoding plasmid, and 200 ng each of two pegRNA- or sgRNA-encoding plasmids) using 1.5 μL Lipofectamine 2000 (Life Technologies). The GFP-positive cells were analyzed by flow cytometry and fluorescence microscopy 72 h after transfection. For endogenous mutagenesis, HEK293T cells were seeded onto 24-well plates and transfected with appropriate plasmids (for the PE2 experiments, the PE2-or PE2 nuclease-encoding plasmid [1,500 ng] and the two pegRNA-encoding plasmids [each 250 ng]; for the Cas9 experiments, the Cas9-encoding plasmid [1,500 ng] and the two sgRNA-encoding plasmids [each 250 ng]) using 3 μL Lipofectamine 2000. After 96 h, genomic DNA was isolated with a DNeasy Tissue Kit (Qiagen) according to the manufacturer's instructions. To generate reporter stale cell lines, 2×10^5 HEK293T cells were seeded onto 24-well plates and 500 ng viral vector

Figure 4. Use of PETI to generate cancer-associated inversions

(A) Schematic of chromosome 2 before and after the paracentric inversion generating the *EML4-ALK* fusion. (B) Schematic *of EML4-ALK* fusion variants. *EML4-ALK* variant 1 (V1), variant 2 (V2), and variant 3 (V3) are generated by fusion of *EML4* exon 13 to *ALK* exon 20, *EML4* exon 20 to *ALK* exon 20, and *EML4* exon 6 to *ALK* exon 20, respectively. (C) Representative results of relative frequency of sequence reads in PCR amplicons amplified by inversion-specific primers amplifying either junction-1 or junction-2. (D) Targeted deep sequencing of amplicons generated using inversion-specific primers. The bar charts represent the fraction of reads with direct inversions (blue), PETI-guided inversions (orange), and inversions with unwanted indels (gray). (E) Fraction of sequencing reads of multiplex PCR amplicons generated from desired and undesired PE2-, Cas9 nuclease-, and PE2 nuclease-mediated inversions. (F) Sequence chromatogram of a region of the *EML4-ALK* fusion transcripts showing the correct *EML4-ALK* junctions. (G and H) Flow cytometry analysis to estimate the percentage of cells with *EML4-ALK* V2 rearrangement by Cas9 and PE2 nuclease. p values were derived from Student's two-tailed t test. Data are presented as mean ± SEM (n = 3 biologically independent samples).

(pLX-TL-mcherry and pLX-TL-eEGFP), 300 ng plasmids of psPAX2, and 200 ng plasmids of pMD2.G were transfected one day after cell seeding. Medium was changed 24 h after transfection, and supernatant containing viral particle was harvested 72 h after transfection. The virus particle was filtered using a 0.45 μm filter and stored at −70°C until used. Serially diluted virus particle from pLX-TL-mcherry vector was infected in HEK293T cells, and puromycin was treated 24 h after infection for 3 days. Then, virus particle from pLX-TL-eEGFP vectors was transduced in these cells and blasticidin was treated 24 h after transduction for 3 days. Cells with one copy of pLX-TL-mcherry and pLX-TL-eGFP cassette were selected to stable cell reporter assay.

Multiplex PCR and sequencing

Targeted genomic sites were amplified using four primers, which could amplify not only sequences from wild-type chromosomes but also the junctions of rearranged genomic regions, and Phusion polymerase (New England BioLabs). To produce sequencing libraries, the resulting PCR amplicons were ligated with NEBNext Adaptors (New England BioLabs) and amplified using NEBNext Multiplex Oligos for Illumina (New England BioLabs) according to the manufacturer's instructions. Sequencing libraries were then subjected to paired-end sequencing using an Illumina sequencing platform (iSeq or MiSeq).

RNA extraction and RT-PCR

RT-PCR was performed to amplify oncogenic fusion transcripts. Total RNA was extracted from transfected cells with a RNeasy Mini Kit (Qiagen) according to the manufacturer's instructions. Total RNA (1 μg) was reverse transcribed using the TOPscript cDNA Synthesis Kit (Enzynomics) according to the manufacturer's instructions. PCR amplification was performed using Taq DNA Polymerase (Life Technologies), and PCR products were analyzed by gel electrophoresis.

Intracellular staining of ALK proteins and flow cytometry

Cells were washed in phosphate-buffered saline twice, resuspended in 4% formaldehyde, and incubated for 15 min at room temperature for fixation. Fixed cells were washed in PBS twice and permeabilized in ice-cold 90% methanol for 30 min in ice. Then, cells were washed in 0.5% BSA and stained with 1:500 anti-ALK (#3633T; Cell Signaling Technology) for 1 h at room temperature, washed in 0.5% BSA, and stained with 1:500 anti-rabbit Alexa Fluor 488 secondary antibody (ab150077; Abcam) for 30 min at room temperature. Cells were washed in 0.5% BSA twice, resuspended in PBS, and analyzed using BD FACSAria II flow cytometry.

Statistical analyses

All results from experiments with two or three independent replicates are expressed as mean ± SEM. p values were calculated using the two-tailed Student's t test.

DATA AVAILABILITY

Sequencing data were deposited in the National Center for Biotechnology Information (NCBI) Sequence Read Archive (SRA) database with BioProject accession code PRJNA804661.

SUPPLEMENTAL INFORMATION

Supplemental information can be found online at https://doi.org/10.1016/j.ymthe.2022.09.008.

ACKNOWLEDGMENTS

This work was supported by grants from the National Research Foundation of Korea (2020R1A2C2101714 to D.K.; 2017M3A9B4062419, 2021R1C1C1007162, and 2018R1A5A2020732 to Y.K.; and 2021R1C1C2013270 to J.K.), the Korean Fund for Regenerative Medicine (KFRM) grant funded by the Korean government (Ministry of Science and ICT, Ministry of Health & Welfare [21A0202L1-12 to D.K.]), and the Korea Health Technology R&D Project through the Korea Health Industry Development Institute (KHIDI), funded by the Ministry of Health & Welfare, Republic of Korea (HI21C1314 to D.K.).

AUTHOR CONTRIBUTIONS

Y.K. and D.K. supervised the research. J.K., H.-Y.H., and H.R. performed the experiments. J.K., Y.K., and D.K. carried out bioinformatics analyses. D.K. and Y.K. wrote the manuscript. All authors approved the manuscript.

DECLARATION OF INTERESTS

The authors declare that they have no competing interests.

REFERENCES

1. Weckselblatt, B., and Rudd, M.K. (2015). Human structural variation: mechanisms of chromosome rearrangements. Trends Genet. *31*, 587–599.
2. Stankiewicz, P., and Lupski, J.R. (2010). Structural variation in the human genome and its role in disease. Annu. Rev. Med. *61*, 437–455.
3. Stratton, M.R., Campbell, P.J., and Futreal, P.A. (2009). The cancer genome. Nature *458*, 719–724.
4. Brunet, E., Simsek, D., Tomishima, M., DeKelver, R., Choi, V.M., Gregory, P., Urnov, F., Weinstock, D.M., and Jasin, M. (2009). Chromosomal translocations induced at specified loci in human stem cells. Proc. Natl. Acad. Sci. USA *106*, 10620–10625.
5. Lee, H.J., Kweon, J., Kim, E., Kim, S., and Kim, J.S. (2012). Targeted chromosomal duplications and inversions in the human genome using zinc finger nucleases. Genome Res. *22*, 539–548.
6. Piganeau, M., Ghezraoui, H., De Cian, A., Guittat, L., Tomishima, M., Perrouault, L., René, O., Katibah, G.E., Zhang, L., Holmes, M.C., et al. (2013). Cancer translocations in human cells induced by zinc finger and TALE nucleases. Genome Res. *23*, 1182–1193.
7. Kim, Y., Kweon, J., Kim, A., Chon, J.K., Yoo, J.Y., Kim, H.J., Kim, S., Lee, C., Jeong, E., Chung, E., et al. (2013). A library of TAL effector nucleases spanning the human genome. Nat. Biotechnol. *31*, 251–258.
8. Maddalo, D., Manchado, E., Concepcion, C.P., Bonetti, C., Vidigal, J.A., Han, Y.C., Ogrodowski, P., Crippa, A., Rekhtman, N., de Stanchina, E., et al. (2014). In vivo engineering of oncogenic chromosomal rearrangements with the CRISPR/Cas9 system. Nature *516*, 423–427.
9. Guo, Y., Xu, Q., Canzio, D., Shou, J., Li, J., Gorkin, D.U., Jung, I., Wu, H., Zhai, Y., Tang, Y., et al. (2015). CRISPR inversion of CTCF sites alters genome topology and enhancer/promoter function. Cell *162*, 900–910.
10. Choi, P.S., and Meyerson, M. (2014). Targeted genomic rearrangements using CRISPR/Cas technology. Nat. Commun. *5*, 3728.
11. Torres, R., Martin, M.C., Garcia, A., Cigudosa, J.C., Ramirez, J.C., and Rodriguez-Perales, S. (2014). Engineering human tumour-associated chromosomal translocations with the RNA-guided CRISPR-Cas9 system. Nat. Commun. *5*, 3964.

12. Ghezraoui, H., Piganeau, M., Renouf, B., Renaud, J.B., Sallmyr, A., Ruis, B., Oh, S., Tomkinson, A.E., Hendrickson, E.A., Giovannangeli, C., et al. (2014). Chromosomal translocations in human cells are generated by canonical nonhomologous end-joining. Mol. Cell *55*, 829–842.

13. Anzalone, A.V., Randolph, P.B., Davis, J.R., Sousa, A.A., Koblan, L.W., Levy, J.M., Chen, P.J., Wilson, C., Newby, G.A., Raguram, A., and Liu, D.R. (2019). Search-and-replace genome editing without double-strand breaks or donor DNA. Nature *576*, 149–157.

14. Lin, Q., Zong, Y., Xue, C., Wang, S., Jin, S., Zhu, Z., Wang, Y., Anzalone, A.V., Raguram, A., Doman, J.L., et al. (2020). Prime genome editing in rice and wheat. Nat. Biotechnol. *38*, 582–585.

15. Liu, Y., Li, X., He, S., Huang, S., Li, C., Chen, Y., Liu, Z., Huang, X., and Wang, X. (2020). Efficient generation of mouse models with the prime editing system. Cell Discov. *6*, 27.

16. Bosch, J.A., Birchak, G., and Perrimon, N. (2021). Precise genome engineering in Drosophila using prime editing. Proc. Natl. Acad. Sci. USA *118*. e2021996118.

17. Petri, K., Zhang, W., Ma, J., Schmidts, A., Lee, H., Horng, J.E., Kim, D.Y., Kurt, I.C., Clement, K., Hsu, J.Y., et al. (2022). CRISPR prime editing with ribonucleoprotein complexes in zebrafish and primary human cells. Nat. Biotechnol. *40*, 189–193.

18. Xu, W., Yang, Y., Yang, B., Krueger, C.J., Xiao, Q., Zhao, S., Zhang, L., Kang, G., Wang, F., Yi, H., et al. (2022). A design optimized prime editor with expanded scope and capability in plants. Nat. Plants *8*, 45–52.

19. Jang, H., Jo, D.H., Cho, C.S., Shin, J.H., Seo, J.H., Yu, G., Gopalappa, R., Kim, D., Cho, S.R., Kim, J.H., and Kim, H.H. (2022). Application of prime editing to the correction of mutations and phenotypes in adult mice with liver and eye diseases. Nat. Biomed. Eng. *6*, 181–194.

20. Zhi, S., Chen, Y., Wu, G., Wen, J., Wu, J., Liu, Q., Li, Y., Kang, R., Hu, S., Wang, J., et al. (2022). Dual-AAV delivering split prime editor system for in vivo genome editing. Mol. Ther. *30*, 283–294.

21. Liu, P., Liang, S.Q., Zheng, C., Mintzer, E., Zhao, Y.G., Ponnienselvan, K., Mir, A., Sontheimer, E.J., Gao, G., Flotte, T.R., et al. (2021). Improved prime editors enable pathogenic allele correction and cancer modelling in adult mice. Nat. Commun. *12*, 2121.

22. Choi, J., Chen, W., Suiter, C.C., Lee, C., Chardon, F.M., Yang, W., Leith, A., Daza, R.M., Martin, B., and Shendure, J. (2022). Precise genomic deletions using paired prime editing. Nat. Biotechnol. *40*, 218–226.

23. Jiang, T., Zhang, X.O., Weng, Z., and Xue, W. (2022). Deletion and replacement of long genomic sequences using prime editing. Nat. Biotechnol. *40*, 227–234.

24. Lee, H.J., Kim, E., and Kim, J.S. (2010). Targeted chromosomal deletions in human cells using zinc finger nucleases. Genome Res. *20*, 81–89.

25. Tucker, J.D. (2010). Chromosome translocations and assessing human exposure to adverse environmental agents. Environ. Mol. Mutagen. *51*, 815–824.

26. Hallberg, B., and Palmer, R.H. (2016). The role of the ALK receptor in cancer biology. Ann. Oncol. *27*, iii4–iii15.

27. Zhang, S.S., Nagasaka, M., Zhu, V.W., and Ou, S.H.I. (2021). Going beneath the tip of the iceberg. Identifying and understanding EML4-ALK variants and TP53 mutations to optimize treatment of ALK fusion positive (ALK+) NSCLC. Lung Cancer *158*, 126–136.

28. Chmielecki, J., Crago, A.M., Rosenberg, M., O'Connor, R., Walker, S.R., Ambrogio, L., Auclair, D., McKenna, A., Heinrich, M.C., Frank, D.A., and Meyerson, M. (2013). Whole-exome sequencing identifies a recurrent NAB2-STAT6 fusion in solitary fibrous tumors. Nat. Genet. *45*, 131–132.

29. Anzalone, A.V., Gao, X.D., Podracky, C.J., Nelson, A.T., Koblan, L.W., Raguram, A., Levy, J.M., Mercer, J.A.M., and Liu, D.R. (2022). Programmable deletion, replacement, integration and inversion of large DNA sequences with twin prime editing. Nat. Biotechnol. *40*, 731–740.

30. Kweon, J., Yoon, J.K., Jang, A.H., Shin, H.R., See, J.E., Jang, G., Kim, J.I., and Kim, Y. (2021). Engineered prime editors with PAM flexibility. Mol. Ther. *29*, 2001–2007.

YMTHE, Volume *31*

Supplemental Information

Targeted genomic translocations and inversions generated using a paired prime editing strategy

Jiyeon Kweon, Hye-Yeon Hwang, Haesun Ryu, An-Hee Jang, Daesik Kim, and Yongsub Kim

Figure S1. Analysis of Cas9-mediated DNA recombination in episomal reporter system.

Targeted sequencing results of amplicons generated using recombination-specific primers.

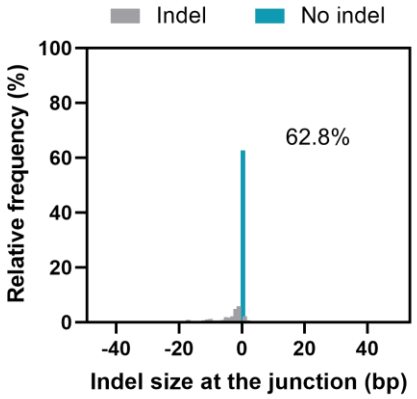


```
Direct junction
GATCCGGCACTGCGGCTGGAGGCGTGCTCAGTCTGGGCCAGCCAC Ref. (total: 5744)
GATCCGGCACTGCGGCTGGAGGCGTGCTCAGTCTGGGCCAGCCAC   3211 (55.9%)
GATCCGGCACTGCGGCTGGAGG-GTGCTCAGTCTGGGCCAGCCAC    223  (3.8%)
GATCCGGCACTGCGGCTGGAG--GTGCTCAGTCTGGGCCAGCCAC    213  (3.7%)
GATCCGGCACTGCGGCTGGAG----GCTCAGTCTGGGCCAGCCAC     67  (1.2%)
GATCCGGCACTGCGGCTGGA-GCGTGCTCAGTCTGGGCCAGCCAC     62  (1.1%)
GATCCGGCACTGCGGCTGGAGGACGTGCTCAGTCTGGGCCAGCCA     46  (0.8%)
GATCCGGCACTGCGGCTGGGGG---GCTCAGTCTGGGCCAGCCAC     45  (0.7%)D
```

Figure S2. Analysis of PETI-mediated genomic translocation in reporter integrated cells.
Targeted sequencing results of amplicons generated using translocation-specific primers.

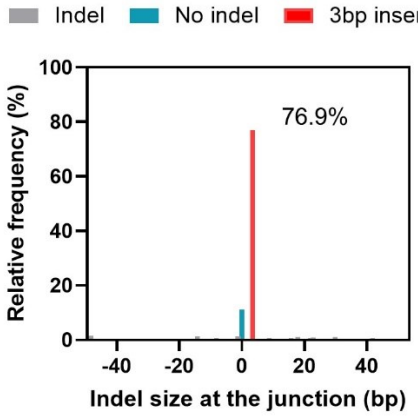

3bp insertion

```
GATCCGGCACTGCGGCTGGAGG---CGTGCTCAGTCTGGGCCAGCCAC Ref. (total: 10680)
GATCCGGCACTGCGGCTGGAGGACGCGTGCTCAGTCTGGGCCAGCCAC   6916 (64.8%)
GATCCGGCACTGCGGCTGGAGG---CGTGCTCAGTCTGGGCCAGCCAC   1002  (9.4%)
GATCCGGCAC----------------TGCTCAGTCTGGGCCAGCCAC    135  (1.3%)
GATCCGGCACTGCGGCTGGAGG----GTGCTCAGTCTGGGCCAGCCAC    115  (1.1%)
GATCCGGCACTGCGGCTGGAGG----------GTCTGGGCCAGCCAC     67  (0.6%)
```

Figure S3. PCR assay for HEK3-HEK4 translocations in HEK293T cells. (a) PCR products were amplified by translocation-specific primers, either H3F (HEK3 forward) and H4R (HEK4 reverse) or H4F (HEK4 forward) and H3R (HEK3 reverse). (b,c) PE2-nuclease mediated insertion of a restriction enzyme site at translocation junctions.

a

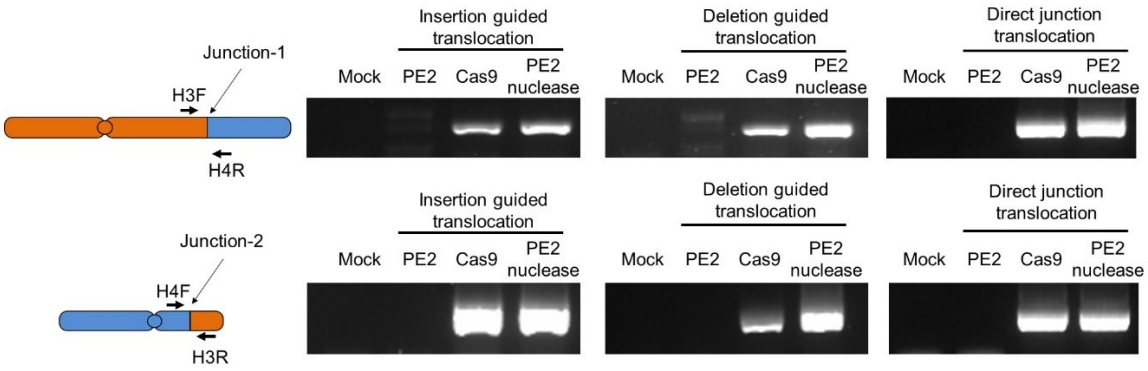

b

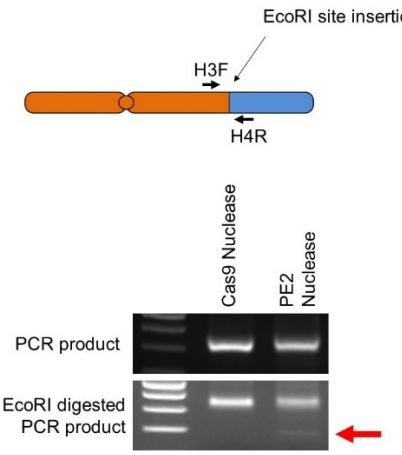

c

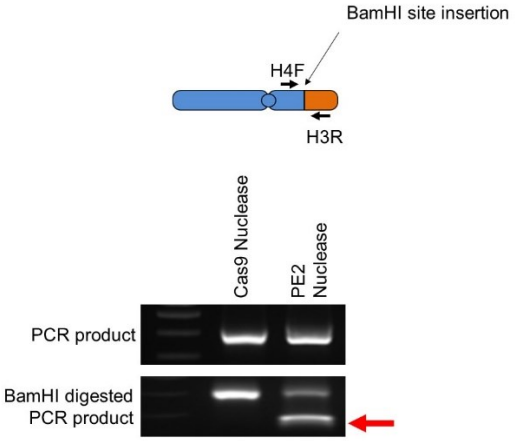

Figure S4. Estimation of HEK3-HEK4 translocation frequencies. The frequencies of translocations were estimated by digital PCR analysis using serially diluted samples. Genomic DNA samples isolated from Cas9 or PE2 nuclease treated cells were serially diluted in distilled water and diluted samples were then subjected to nested PCR using appropriate primers. Critical dilution points that support the amplification of breakpoint junctions were determined. The results were analyzed using the Extreme Limiting Dilution Analysis program (http://bioinf.wehi.edu.au/software/elda/).[1]

Dosage	Cas9				PE2 nuclesae											
					Insertion guided				Deletion guided				Direct junction guided			
	Junction-1		Junction-2		Junction-1		Junction-2		Junction-1		Junction-2		Junction-1		Junction-2	
pg	Tested	Response	Tested	Response	Tested	Response	Tested	Response	Tested	Response	Tested	Response	Tested	Response	Tested	Response
66	12	1	12	1	12	0	12	0	12	0	12	0	12	0	12	0
660	24	5	24	9	24	4	24	12	24	2	24	11	24	2	24	4
3300	12	6	12	9	12	5	12	10	12	4	12	12	12	7	12	8

Figure S5. Types of translocations induced by DNA DSBs. Schematic of the chromosomal translocations induced by DNA DSBs. When two DSBs are induced simultaneously in different chromosomes, translocations can cause four different types of genomic rearrangements, two of reciprocal translocations, dicentric chromosome, acentric chromosome.

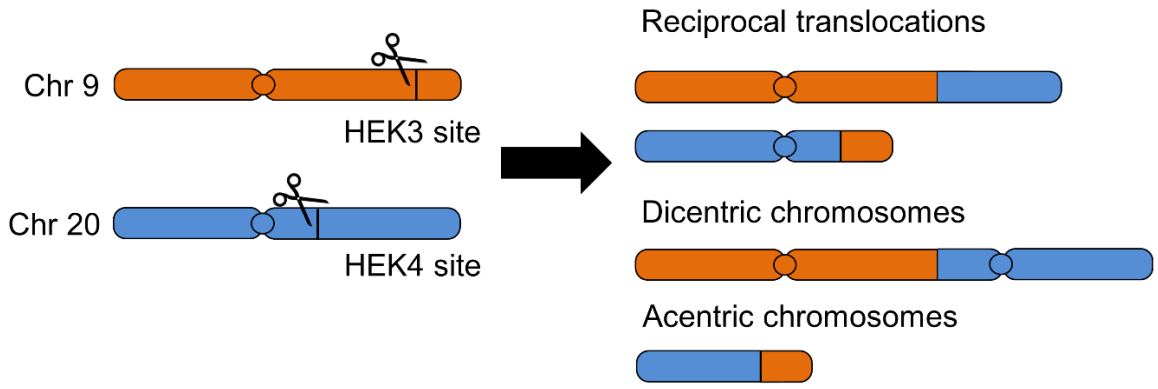

Figure S6. Off-target analysis of HEK3 and HEK4 target sites. Mutation frequencies induced by PE2, PE2 nuclease, or Cas9 nuclease at the HEK3 and HEK4 on- and off-target sites.

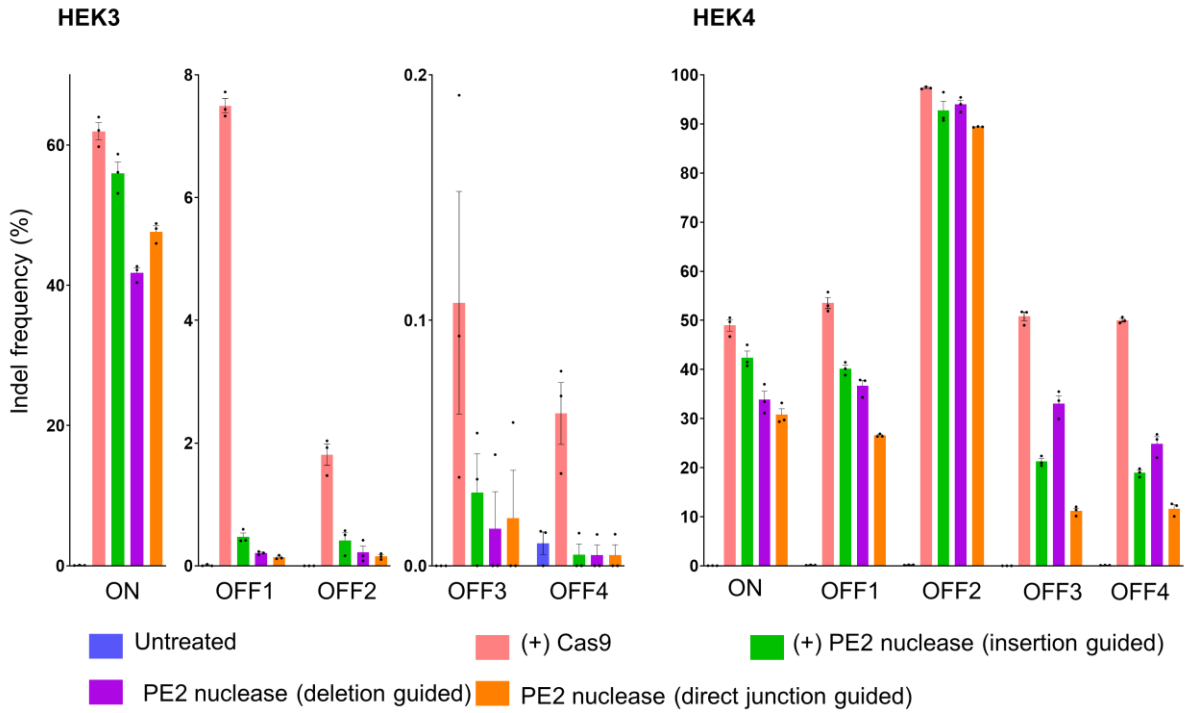

ON	GGCCCAGACTGAGCACGTGATGG
OFF1	caCCCAGACTGAGCACGTGcTGG
OFF2	aGCtCAGACTGAGCAaGTGAGGG
OFF3	GagCCAGAaTGAGCACGTGAGGG
OFF4	GGCCCAGACTGAGCAaaaGAAGG

ON	GGCACTGCGGCTGGAGGTGGGGG
OFF1	GGCAaTGCGGCTGGAGGcGGAGG
OFF2	GGCACgaCGGCTGGAGGTGGGGG
OFF3	GGCACTGCtGCTGGgGGTGGTGG
OFF4	aGCAgTGCGGCTaGAGGTGGTGG

Figure S7. Estimation of translocation frequencies between HEK3 on-target site and HEK4 off-target sites. The frequencies of translocations between HEK3 on-target site and HEK4 off-target sites were estimated by digital PCR analysis as mentioned in Supplementary Figure 4.

Dosage	HEK3 - HEK4 OFF1								HEK3 - HEK4 OFF2							
	Cas9				PE2 nuclease				Cas9				PE2 nuclease			
	Junction-1		Junction-2		Junction-1		Junction-2		Junction-1		Junction-2		Junction-1		Junction-2	
pg	Tested	Response	Tested	Response	Tested	Response	Tested	Response	Tested	Response	Tested	Response	Tested	Response	Tested	Response
20000	1	1	1	1	5	4	1	1	-	-	-	-	4	3	4	4
10000	1	1	1	1	5	3	1	1	5	5	5	5	5	2	5	3
5000	5	4	1	1	5	1	5	4	5	4	5	5	5	1	5	2
2500	5	3	5	5	1	0	5	1	5	2	5	2	5	0	5	0
1250	5	3	5	2	1	0	5	0	5	1	5	2	1	0	1	0
625	1	0	5	0	1	0	1	0	1	1	1	0	1	0	1	0
313	1	0	1	0	1	0	1	0	1	0	1	0	1	0	1	0
156	1	0	1	0	1	0	1	0	1	0	1	0	1	0	1	0
78	-	-	-	-	-	-	-	-	1	0	1	0	1	0	1	0

Figure S8. PCR assay for *NPM1-ALK* and *KIF5B-ALK* translocations in HEK293T cells. (a,b) Detection of PE2-, Cas9 nuclease-, or PE2 nuclease-mediated translocations using translocation-specific primers. (c) Schematic of the *NPM1-ALK* fusion transcript (left). Detection of the *NPM1-ALK* fusion transcript by RT-PCR using total RNA as template (right).

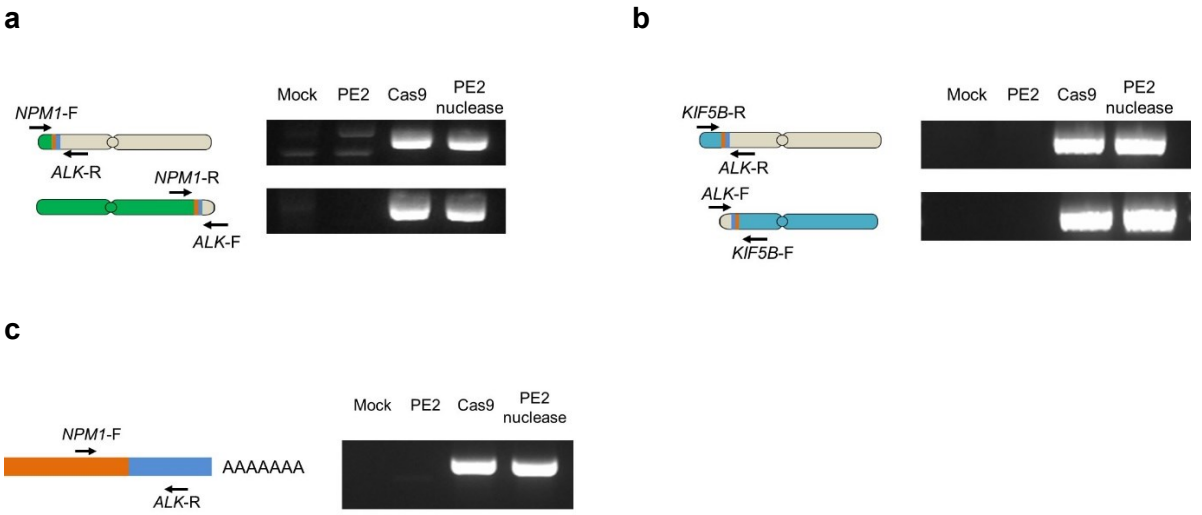

Figure S9. Estimation of *NPM1-ALK* and *KIF5B-ALK* translocation frequencies. The frequencies of *NPM1-ALK* or *KIF5B-ALK* translocations were estimated by digital PCR analysis as mentioned in Supplementary Figure 4.

Dosage	*NPM1-ALK*							
	Cas9				PE2 nuclease			
	Junction-1		Junction-2		Junction-1		Junction-2	
pg	Tested	Response	Tested	Response	Tested	Response	Tested	Response
20000	1	1	1	1	1	1	1	1
10000	5	4	1	1	1	1	1	1
5000	5	2	5	4	1	1	5	5
2500	5	1	5	2	1	1	5	4
1250	1	0	5	0	5	5	5	2
625	1	0	1	0	5	5	1	0
313	1	0	1	0	5	2	1	0
156	1	0	1	0	1	0	1	0
78	-	-	-	-	-	-	-	-

Dosage	*KIF5B-ALK*							
	Cas9				PE2 nuclease			
	Junction-1		Junction-2		Junction-1		Junction-2	
pg	Tested	Response	Tested	Response	Tested	Response	Tested	Response
30000	1	1	1	1	1	1	1	1
15000	5	5	1	1	1	1	1	1
7500	5	3	5	4	5	4	5	4
3750	5	0	5	1	5	3	5	1
1875	1	0	5	0	5	1	5	0
938	1	0	1	0	1	0	1	0
469	1	0	1	0	1	0	1	0
234	1	0	1	0	1	0	1	0
117	-	-	-	-	-	-	-	-

Figure S10. Chromosomal rearrangements in A549 cell lines. (a) Sequencing results of targeted amplicon amplified using translocation-specific primers in A549 cells. (b) Sequencing results of targeted amplicon amplified using inversion-specific primers in A549 cells.

a

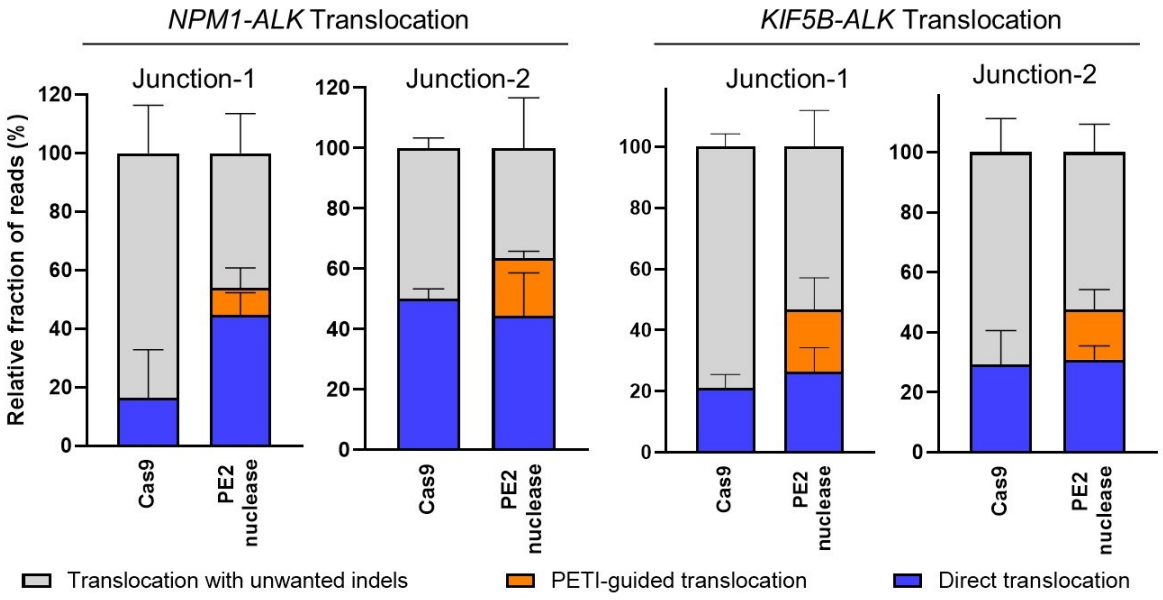

b

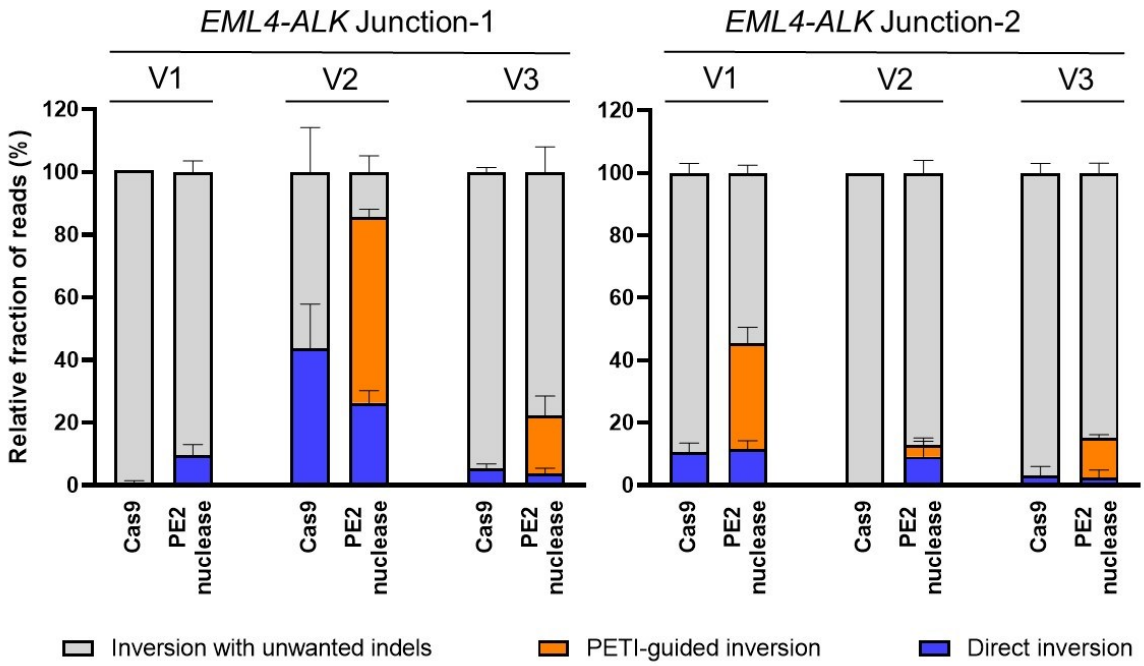

Figure S11. PCR assay for three types of *EML4-ALK* inversions in HEK293T cells. (a) PCR assay for inversions. Products were amplified by inversion-specific primers. (b) Detection of the *EML4-ALK* fusion transcript by RT-PCR using inversion-specific primers. Total RNA from HEK293T cells transfected with plasmids encoding PE2, Cas9 nuclease, or PE2 nuclease was used as template.

a

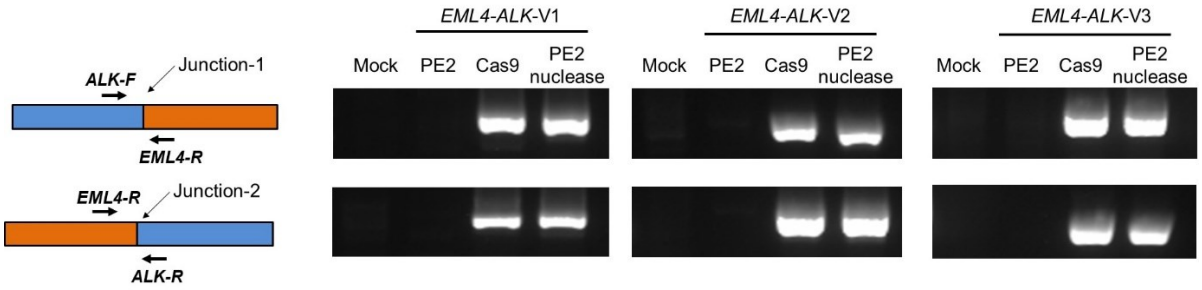

b

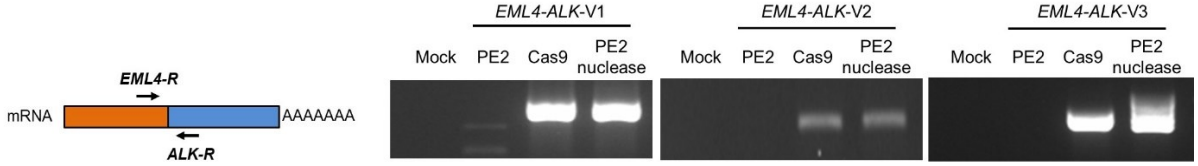

Figure S12. Estimation of three types of *EML4-ALK* inversions frequencies. The frequencies of inversions were estimated by digital PCR analysis as mentioned in Supplementary Figure 4.

Dosage	*EML4-ALK*-V1								*EML4-ALK*-V2								*EML4-ALK*-V3							
	Cas9				PE2 nuclease				Cas9				PE2 nuclease				Cas9				PE2 nuclease			
	Junction-1		Junction-2		Junction-1		Junction-2		Junction-1		Junction-2		Junction-1		Junction-2		Junction-1		Junction-2		Junction-1		Junction-2	
pg	Tested	Response	Tested	Response	Tested	Response	Tested	Response	Tested	Response	Tested	Response	Tested	Response	Tested	Response	Tested	Response	Tested	Response	Tested	Response	Tested	Response
20000	-	-	-	-	-	-	-	-	-	-	-	-	1	1	1	1	-	-	-	-	-	-	-	-
10000	1	1	1	1	1	1	1	1	1	1	1	1	1	1	1	1	1	1	1	1	1	1	1	1
5000	1	1	1	1	1	1	1	1	1	1	1	1	1	1	1	1	1	1	1	1	1	1	1	1
2500	1	1	1	1	1	1	1	1	1	1	1	1	1	1	1	1	1	1	1	1	1	1	1	1
1250	5	4	5	4	5	5	1	1	1	1	1	1	1	1	1	1	5	5	5	3	1	1	5	4
625	5	1	5	1	5	4	1	1	1	1	1	1	1	1	1	1	5	2	5	2	1	1	5	3
313	5	0	5	1	5	1	5	4	5	4	1	1	1	1	1	1	5	0	5	0	5	4	5	0
156	1	0	1	0	1	0	5	1	5	1	5	4	5	5	1	1	1	0	1	0	5	1	1	0
78	1	0	1	0	1	0	5	0	5	0	5	2	5	4	5	5	1	0	1	0	5	0	1	0
39	-	-	-	-	-	-	-	-	1	0	5	1	5	1	5	2	-	-	-	-	-	-	-	-
20	-	-	-	-	-	-	-	-	1	0	1	0	1	0	5	0	-	-	-	-	-	-	-	-
10	-	-	-	-	-	-	-	-	1	0	1	0	1	0	1	0	-	-	-	-	-	-	-	-
5	-	-	-	-	-	-	-	-	1	0	1	0	-	-	-	-	-	-	-	-	-	-	-	-

Figure S13. Analysis of PETI-mediated chromosomal translocation and inversion with various length of RTT in each pegRNAs. (a) Targeted deep sequencing results of amplicons generated using HEK3-HEK4 translocation-specific primers. (b) Targeted sequencing results of amplicons generated using *EML4-ALK* translocation-specific primers.

a

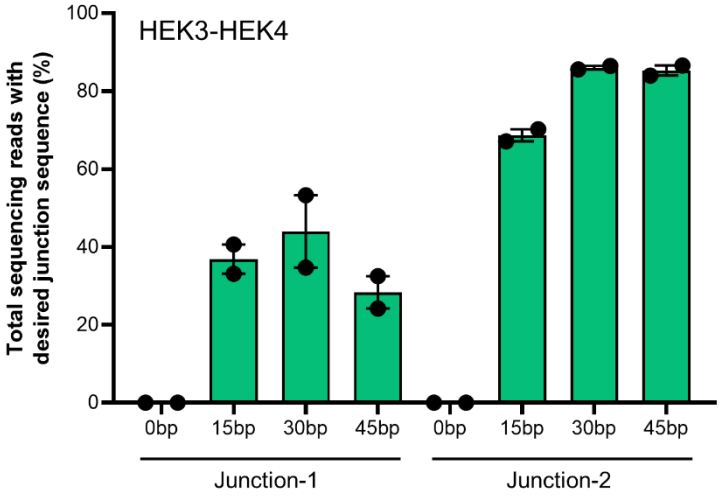

b

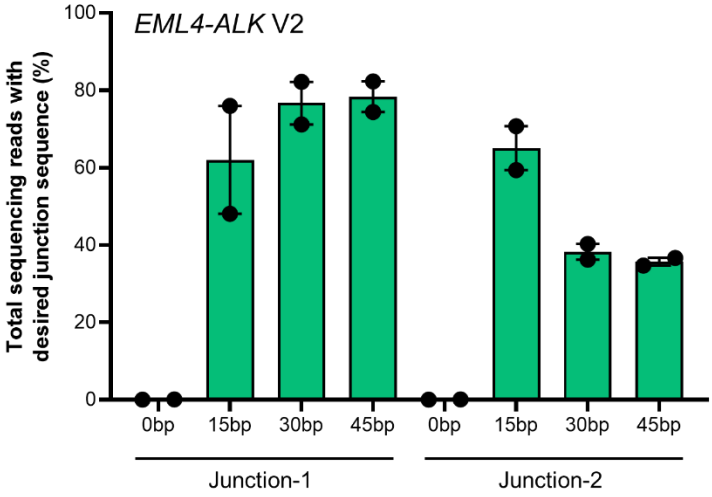

Figure S14. PCR assay for insertion of attP site at translocation junctions in HEK293T cells.

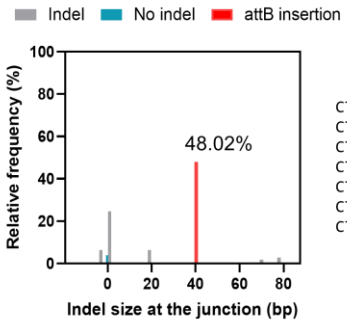


```
CTTGCTATATCCTCGA----------------------------------------CGATGGTGAAAGCTCG Ref. (total: 16986)
CTTGCTATATCCTCGACGGCTTGTCGACGACGGCGGTCTCCGTCGTCAGGATCATCCGATGGTGAAAGCTCG  8214 (48.36%)
CTTGCTATATCCTCGAA---------------------------------------CGATGGTGAAAGCTC  4264 (25.10%)
CTTGCTATATCCT-------------------------------------------CGATGGTGAAAGCTCG  1094  (6.44%)
CTTGCTATAGGAAGAGATGAATCCTGCACCAGCCCCCAGCTTTCTTC---------CGATGGTGAAAGCTCG  1041  (6.13%)
CTTGCTATATCCTCGA----------------------------------------CGATGGTGAAAGCTCG   693  (4.08%)
CTTGCTATATCCTCGAAAG-------------------------------------CGATGGTGAAAGCTCG   663  (3.90%)
```

Table S1. Sequences of pegRNAs used in the experiments.

pegRNA name	Target gene	RT-name	Spacer sequence		PBS (5' to 3', 13 nt)	RTT sequence (5' to 3')
HEK3-E1	HEK3	E-HEK4-Perfect	ggcccagactgagcacgtga	TGG	cagactgagcacg	tgggggttaaagcggagactctggtgctgt
HEK3-E2	HEK3	E-HEK4-EcoRI-ins	ggcccagactgagcacgtga	TGG	cagactgagcacg	AATTCtgggggttaaagcggagactctggtgctgt
HEK3-E3	HEK3	E-HEK4-3bp-del	ggcccagactgagcacgtga	TGG	cagactgagcacg	gggttaaagcggagactctggtgctgtgtg
HEK4-E1	HEK4	E-HEK3-Perfect	ggcactgcggctggaggtgg	GGG	ctgcggctggagg	tgatggcagaggaaaggaaggaagccctgcttcc
HEK4-E2	HEK4	E-HEK3-BamHI-ins	ggcactgcggctggaggtgg	GGG	ctgcggctggagg	ATCCtgatggcagaggaaaggaaggaagccctgcttcc
HEK4-E3	HEK4	E-HEK3-3bp-del	ggcactgcggctggaggtgg	GGG	ctgcggctggagg	tggcagaggaaaggaagccctgcttcctcc
ALK-V1	ALK	ALK-1-BamHI-EXT	gcgagctttcaccatcgtga	TGG	gctttcaccatcg	GGATCCtgatggctaaataacagcccagttttcttg
EML4-V1	EML4	EML4-2-EcoRI-EXT	attcagctgtaccaatgtga	TGG	agctgtaccaatg	GAATTCtgatggacactgaaggagctccccaccccc
ALK-V2	ALK	ALK-EML4-V2(EcoRI)-EXT	tccttcagtgtccatcacga	TGG	tcagtgtccatca	GAATTctaaggtaatgagaatctcaaatgtgattc
ELM4-V2	EML4	EML4-V2(BamHI)-EXT	gcatatgttatgctgagcta	AGG	atgttatgctgag	GGATCCcgatggtgaaagctcgcccccaccctaga
ALK-NPM1	ALK	ALK-NPM1(BamHI)-EXT	gcgagctttcaccatcgtga	TGG	gctttcaccatcg	GATCCtcgaggatatagcaagctatgatcacatca
NPM1	NPM1	NPM1(EcoRI)-EXT	gtgaacccagtagcagttcg	AGG	acccagtagcagt	GAATTCtgatggacactgaaggagctccccaccccc
ALK-V3	ALK	ALK-EML4-V3(BamHI)-EXT	gcgagctttcaccatcgtga	TGG	gctttcaccatcg	GATCCtcctggctacagctaatcacaaattttagc
EML4-V3	EML4	EML4-V3(EcoRI)-EXT	tgatcaaccgcaactcttcc	TGG	caaccgcaactct	GAATTCtgatggacactgaaggagctccccaccccc

References

1. Hu, Y, and Smyth, GK (2009). ELDA: extreme limiting dilution analysis for comparing depleted and enriched populations in stem cell and other assays. *J Immunol Methods* **347**: 70-78.